Geomorphology 268 (2016) 177–183

Contents lists available at ScienceDirect

Geomorphology

journal homepage: www.elsevier.com/locate/geomorph

Reduction in soil aggregation in response to dust emission processes

Nitzan Swet *, Itzhak Katra

Department of Geography and Environmental Development, Ben Gurion University of the Negev, Be'er-Sheva, Israel

ARTICLE INFO

Article history:
Received 21 September 2015
Received in revised form 31 May 2016
Accepted 5 June 2016
Available online 07 June 2016

Keywords:
Soil aggregation
Saltation
Aeolian erosion
Dust
PM_{10}

ABSTRACT

Dust emission by aeolian (wind) soil erosion depends on the topsoil properties of the source area, especially on the nature of the aggregates where most dust particles are held. Although the key role of soil aggregates in dust emission, the response of soil aggregation to aeolian processes and its implications for dust emission remain unknown. This study focuses on aggregate size distribution (ASD) analyses before and after in-situ aeolian experiments in semiarid loess soils that are associated with dust emission. Wind tunnel simulations show that particulate matter (PM) emission and saltation rates depend on the initial ASD and shear velocity. Under all initial ASD conditions, the content of saltator-sized aggregates (63–250 μm) increased by 10–34% due to erosion of macro-aggregates (>500 μm), resulting in a higher size ratio (SR) between the saltators and macro-aggregates following the aeolian erosion. The results revealed that the saltator production increases significantly for soils that are subjected to short-term (anthropogenic) disturbance of the topsoil. The findings highlight a decrease in soil aggregation for all initial ASD's in response to aeolian erosion, and consequently its influence on the dust emission potential. Changes in ASD should be considered as a key parameter in dust emission models of complex surfaces.

1. Introduction

Aeolian (wind) dust emission has a major impact on a variety of environmental and socioeconomic issues. Airborne dust particles can affect climate, biogeochemical cycles, ecosystem productivity, and other components of the Earth system. Dust emission is a major cause of soil loss in arid and semi-arid regions throughout the world (Ravi et al., 2011; Zobeck et al., 2013; Tanner et al., 2016). The loss of nutrients and clays reduces the soil fertility, leading to soil degradation and desertification. In addition, dust events significantly increase air pollution and thus can impact human health (Krasnov et al., 2015; Vodonos et al., 2015). In recent years more soils have become associated with dust emission following anthropogenic activities and disturbance of the topsoil aggregation.

The ability of the topsoil to resist erosion depends on its physicochemical properties, especially on the soil aggregation (Bissonnais, 1996; Hevia et al., 2007; Wang et al., 2014). Soil aggregation refers to the arrangement of solids and void spaces and the bonding materials (mineral and organic) between the particles (Boix-Fayos et al., 2001). Common cementing agents, including clays, organic matter and carbonates, control the aggregate formation and sizes. Aggregate sizes can range between less than 2 μm to a few centimeters in diameter (Tisdall and Oades, 1982; Horn et al., 1994). Changes in external factors, such as climatic conditions and land uses, alter the topsoil properties and thus influence aggregate size and soil erodibility (Lavee et al., 1998; Sharratt et al., 2010; Webb and Strong, 2011; Singh et al., 2012 Tanner et al., 2016). It is generally assumed that soils with a higher amount of large aggregates have stronger resistance against erosion due to their weight (Amézketa, 1999). Only a few studies have referred to the soil aggregation in aeolian processes, but with a focus on the wind erodible fraction - EF that considers only the aggregate size (<840 μm) (Bagnold, 1941; Zobeck et al., 2013). Quantitative information on aggregate strength and stability in wind erosion processes is still lacking.

The emission of dust particles <70 μm from soils is fundamentally linked to the suspension transport mechanisms. However these fine particles are usually part of the soil aggregates and thereby are not available for direct suspension (Ravi et al., 2011). In this case the emission of the fine particles may be enabled by saltation of sand particles and/or aggregates (Shao et al., 1993). The soil aggregates can breakdown to release dust particles either by self-saltating or by the impact of other saltators (Shao, 2008; Kok et al., 2012). Breakdown of larger aggregates during saltation can be explained by the aggregation hierarchy concept, in which macro-aggregates are bonded together from smaller aggregates with weak inter-connections (Tisdall and Oades, 1982; Six et al., 2004).

There are positive relationships between the content of saltators (sand and/or sand-sized aggregates), saltation rates, and dust emission (Shao et al., 1993; Rice et al., 1997; Sweeney et al., 2011; Tanner et al., 2016). Houser and Nickling (2001) showed a short-term direct emission of loose fine particles from the surface, while the increase in

* Corresponding author.
E-mail addresses: swet@post.bgu.ac.il (N. Swet), katra@bgu.ac.il (I. Katra).

http://dx.doi.org/10.1016/j.geomorph.2016.06.002
0169-555X/

saltation flux increases the dust emission rates over time. Abulaiti et al. (2014) found an increase in dust emission rates of up to 8 fold in response to entrainment of saltation. Despite the association between sand flux and dust emission, there is a lack in studies that empirically examined how dust is emitted from aggregates during saltation.

We can assume here that aggregate breakdown will lead to reduction in the aggregate size distribution (ASD), increase in saltation fluxes during erosion, and thereby change the dust production over time. This can affect the dust emission potential over time and in the next wind event. The aim of this study is to quantify changes in the ASD under different initial soil conditions and wind shear velocities to determine the influence of aeolian erosion on soil ASD and thus on the dust emission potential. A semiarid loess soil subjected to long and short-term topsoil disturbances which is associated with dust emissions was analyzed along with in-situ aeolian simulations. A recent study in these soils clearly demonstrated the impact of topsoil properties on dust fluxes through using soil parametrization in a numerical model (Katra et al., 2016). The current study will enable a better understanding of the role of topsoil aggregation in dust emissions, aiming to reduce uncertainties which exist in dust emission models.

2. Materials and methods

2.1. Experimental set up

The experiments were performed on a semi-arid loess soil in the northern Negev, Israel (Fig. 1). Basic differences in soil aggregation are related to long-term influences of land uses – grazing soil (G_L) compared with natural soil (N_L). The G_L soil is characterized mainly by bare surfaces with small patches of dwarf shrubs and sparse herbaceous cover. The N_L is confined within a closed area (military base) without human interference during recent decades. The surface is characterized by patches of biological crust, and annual and seasonal vegetation. A total of 36 samples (18 replicates for each soil) were collected from dry topsoils (0–2 cm) for the analysis of physicochemical properties including aggregate size distribution (ASD) (Section 2.2, Table 1).

In order to form a scale of initial aggregate conditions, the N_L and G_L soils were treated in the field to simulate a short-term disturbance caused by human activities that are common in semi-arid soils. The topsoils were artificially disturbed by mechanical operation of a handheld grading rake (Bacon et al., 2011) and footsteps. Thus N_S and G_S represent a reduced soil aggregation state of the original soils N_L and G_L, respectively. A total of 36 samples (18 replicates for each soil) were taken from the treated topsoils. The samples were analyzed only for ASD, considering that no changes in other physicochemical properties are expected following such a short-term treatment.

After the aeolian experiments (Section 2.3) for the four different initial soil conditions (N_L, G_L, N_S, and G_S), the topsoils were analyzed for ASD to determine the impact of wind erosion under two wind shear velocities (Fig. 1D) with 6 replicates for each soil condition (a total of 48 aeolian experiments). Statistical analyses were applied to determine differences in soil properties and aeolian parameters including means, standard deviations, and significances ($P \le 0.05$) by *t*-test and ANOVA using IBM SPSS Statistics 20.0 software (Corp I.B.M, 2011).

2.2. Soil analyses

The soil samples were tested using standard and advanced soil science methods (Klute, 1986; Rowell, 1994; Pansu and Gautheyrou, 2006) as follows. Aggregate Size Distribution (ASD) was derived using the dry sieving method. The samples were placed on a set of six sieves in diameters (μm) of 63, 125, 250, 500, 1000, and 2000, and were shaken at moderate amplitude of 50 rpm for 8 min on an electronic sieving apparatus with horizontal and vertical motions (RETSCH AS 300 Control, Germany) to avoid aggregate breakdown. After sifting, every size fraction was weighted separately. In the fraction of >2000 μm, rock fragments were extracted from the rest of the soil particles. The results were used to calculate mean weight diameter (MWD) and size ratio (SR)

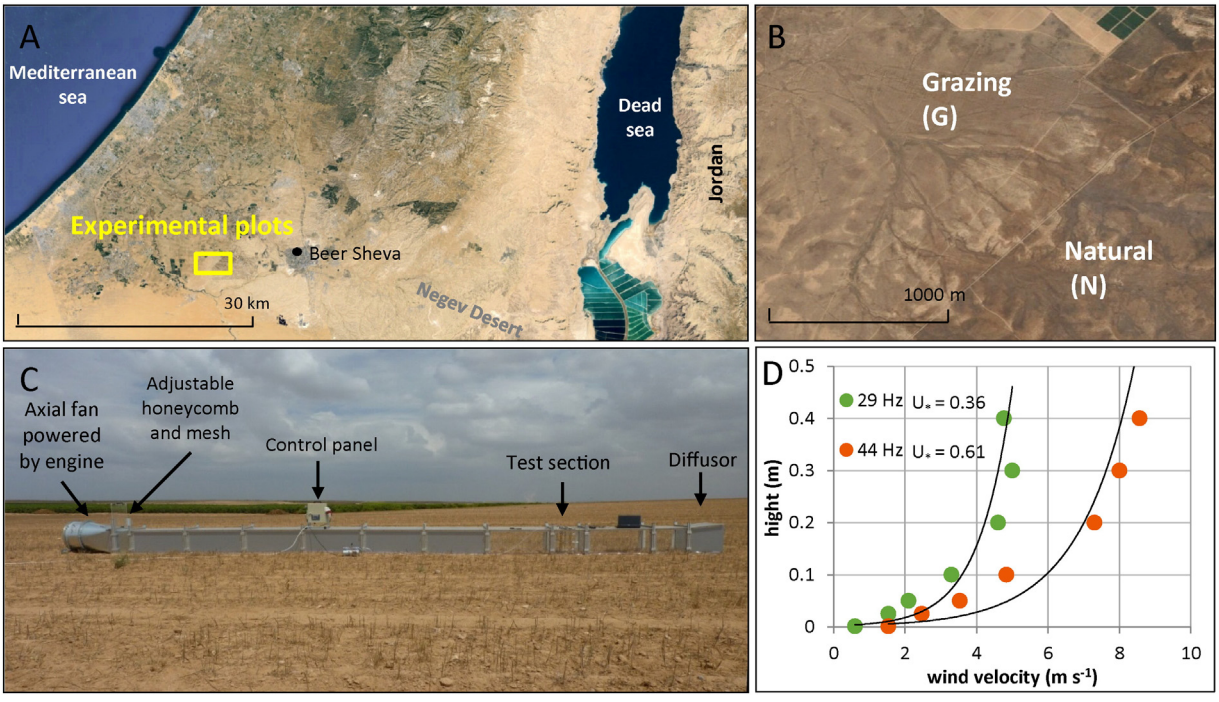

Fig. 1. (A) Location of the experimental soils in the northwestern Negev, Israel. The annual average rainfall is ~200 mm. The dry season extends from April to October with rare rainfall events. Winds are mainly western and can exceed 11 m s^{-1} (at 10-m height). (B) The silt-loam (USDA) soils in natural and grazing areas. (C) The BGU portable wind tunnel used for field experiments on dust emission processes. (D) Wind profile and shear velocities (u_*) measured in the field for fan frequencies of 29 Hz and 44 Hz (maximum velocities of ~5 m s^{-1} and ~9 m s^{-1}, respectively).

Table 1
Mean contents of topsoil properties due to long-term impact in natural (N) and grazing (G) soils, presented as w/w percentages: soil organic matter (SOM), carbonates ($CaCO_3$), clay (<2 μm), fine silt fractions (2–10 μm, 10–20 μm), and sand 50–250 μm. S.D values are in brackets.

	SOM	$CaCO_3$	<2 μm	2–10 μm	10–20 μm	63–250 μm
N	2.28 (0.7)	22.42 (3.7)	12.01 (3.0)	29.86 (3.0)	12.10 (2.5)	18.45 (7.1)
G	1.90 (0.8)	12.13 (2.3)	8.95 (1.6)	21.72 (1.9)	10.12 (3.2)	33.67 (4.5)

calculated as the content of saltators (63–250 μm) divided by the content of macro-aggregates (>500 μm).

Particle size distribution (PSD) was derived by ANALYSETTE 22 MicroTec Plus (Fritsch) laser diffraction, which measures particles in the size range of 0.08–2000 μm. The replicates (100 mg) of each sample were dispersed in Na-hexametaphosphate solution (0.5%) by sonication (38 kHz). PSD data was calculated using the Fraunhofer diffraction model with a size resolution of 1 μm using MasControl software. Soil organic matter (SOM) content (%) was determined by the dry combustion method. A 5 g sample of crushed oven-dried (105 °C for 24 h) soil was placed in a combusting oven at 375 °C for 17 h. At this temperature all soil organic carbon oxidizes with no conflagration of mineral carbon (Wang et al., 2012). Carbonate ($CaCO_3$) was determined as mass content (%) by the Calcimeter device. The carbonates present in a 200 mg sample are converted into CO_2 by adding hydrochloric acid 8% (HCl) to the sample. The calcium carbonate content can be calculated with reference to a standard sample of analytical (100%) $CaCO_3$.

2.3. Aeolian experiments

Aeolian experiments were conducted with a boundary layer wind tunnel (Fig. 1C). Boundary-layer wind tunnels enable aeolian simulations under standardized quasi-natural wind conditions (Leys and Raupach, 1991; Shao, 2008) and provide quantitative information on aeolian particle transport in the field and dust emission rates from soils (Sharratt et al., 2010; Singh et al., 2012; Van Pelt et al., 2013; Zobeck et al., 2013). The wind tunnel has a cross sectional area 0.5 × 0.5 m with open-floored working sections of up to 10 m length (Tanner et al., 2016; Katra et al., 2016). Air push or air suction flow in the tunnel is generated by an axial fan up to a maximum velocity of 18 m s^{-1}. Instruments installed in the test section of the tunnel enable quantification of: (1) wind profile for the calculation of frictional velocity and roughness height (Fig. 1D), (2) saltation impacts, and (3) dust concentrations profile of PM_{10}.

The wind tunnel was operated in the field on bare surfaces of N_L, G_L, N_S, and G_S soils. The tunnel fan was set to two frequencies (29 Hz, 44 Hz), representing wind velocities that are above the threshold of saltators (~5 m s^{-1}), and aeolian erosion (~9 m s^{-1}) in the studied loess soils respectively (Tanner et al., 2016). The calculated shear velocities (u_*) are 0.36 m s^{-1} and 0.61 m s^{-1}, respectively (Fig. 1D). During the aeolian experiments, transport of saltating particles was recorded by a cylindrical piezo-electric sensor (www.sensit.com) that converts the impact energy of the saltating particles (>63 μm) into electrical impulses of number of impacts. The Sensit data were logged on a Campbell Scientific Inc. CR-1000X data logger at 1 second intervals. The concentrations of suspended particles were measured by a real-time dust monitor for background values (DustTrak, TSI). The DustTrak installed in the test section recorded the PM concentration (μg m^{-3}) during each experiment at intervals of 1 s. Each experiment lasted for 600 s, representing a typical trend of soil erosion. A total of 48 experiments were conducted in the field (4 topsoil conditions, 2 wind velocities, 6 replicates). After the aeolian experiments, the soils were sampled for ASD analyses (Section 2.2).

3. Results and discussion

3.1. Initial soil aggregation

The long-term impacts on the soil aggregation (N_L and G_L) are shown by the aggregate size distributions (ASD) results (Fig. 2). N_L soil contains mostly aggregates larger than 2000 μm, while in G_L the highest content was obtained in the aggregate size fraction of 63–125 μm. The calculated MWD was significantly ($P \le 0.05$) higher in N_L (2531.4 μm) than in G_L (1033.6 μm) (Fig. 2). Previous studies have shown a similar trend of decrease in MWD values due to human/grazing activities (Álvaro-Fuentes et al., 2007; Zhang et al., 2012). The significantly ($P \le 0.05$) higher contents of the soil cements (SOM, $CaCO_3$, clay and silt fractions) in N_L compared to G_L (Table 1) can explain the higher aggregation rate and MWD in the natural soils (Pinheiro et al., 2004; Spaccini and Piccolo, 2013). The differences in the soil cements between N_L and G_L are related to the long-term effects of grazing in G plots. Grazing causes a reduction in vegetation cover and topsoil destruction by trampling of the herd, and thus breakdown of soil aggregates and crusts that damages the cohesion of soil particles (Masri et al., 2003). The combination of these two factors leads to higher vulnerability to erosion in the G_L plot (Zaady et al., 2001).

The N_S and G_S soils represent another two initial aggregate conditions formed due to a short-term impact (Fig. 2). In these soils, where topsoil disturbance was simulated by an artificial mechanical operation, a finer ASD was evident, with a reduction in the content of the larger fractions in both soils. In G_S the size fraction 63–250 μm, which is considered to be saltators, was significantly increased due to the disturbance. This resulted in lower MWD values (1811.2 μm in N_S and 673.5 μm in G_S) compared with the long-term implementation in N_L and G_L. The MWD was higher in N_S compared with G_S, due to the more favorable soil properties in N_L (Table 1), although the effect of the short-term impact was similar in both soils (N_S and G_S). Considering that larger aggregates are eroded into saltator-sized fractions, a size ratio (SR) between the contents of saltators (63–250 μm) and macro-aggregates (>500 μm) is used here to scale the initial soil aggregation (Fig. 2) for the aeolian experiments, thus in terms of SR, $N_L < N_S < G_L < G_S$.

3.2. Changes in soil aggregation

The results of the wind tunnel experiments conducted in the field show a distinct pattern in the saltation impacts and PM_{10} concentrations (mg m^{-3}), depending on the initial soil aggregation and the shear velocity (Fig. 3). The grazing soil (G_L) contained more saltators (63–500 μm) and its SR was higher (Fig. 2), which can explain the 2–11 fold higher saltation rates and PM_{10} compared with the natural soil (N_L) (Houser and Nickling, 2001; Sweeney et al., 2008, 2011). In general, the presence of sand-sized aggregates (saltators) in the soil enables the entrainment of dust particles by the ballistic impact during saltation bombardment (Shao et al., 1993). Soils containing larger aggregates are considered as more resistant to aeolian erosion (Hevia et al., 2007; Colazo and Buschiazzo, 2010). In addition higher percentages of cement materials (SOM, $CaCO_3$, clays) that were found in N_L plots compared with G_L plots (Table 1) can indicate a better aggregate stability against breakdown during erosion. The short-term disturbance of the topsoil significantly increased the PM_{10} and saltation rates (up to 6 fold) in both soils (N_S and G_S). Moreover, the amplification of the shear velocity from 0.36 m s^{-1} to 0.61 m s^{-1} led to stronger aeolian erosion under all experimental soil conditions (Fig. 3). These results emphasize the importance of the topsoil aggregation and the strong impact of human activities and short-term disturbance of the topsoil on its resistance against aeolian erosion.

The impact of the aeolian erosion on the soil aggregation was quantified by ASD analyses before and after the aeolian experiments. A reduction in the soil aggregation rate was evident under all experimental conditions in response to erosion (Fig. 4). There was a 10–34% increase

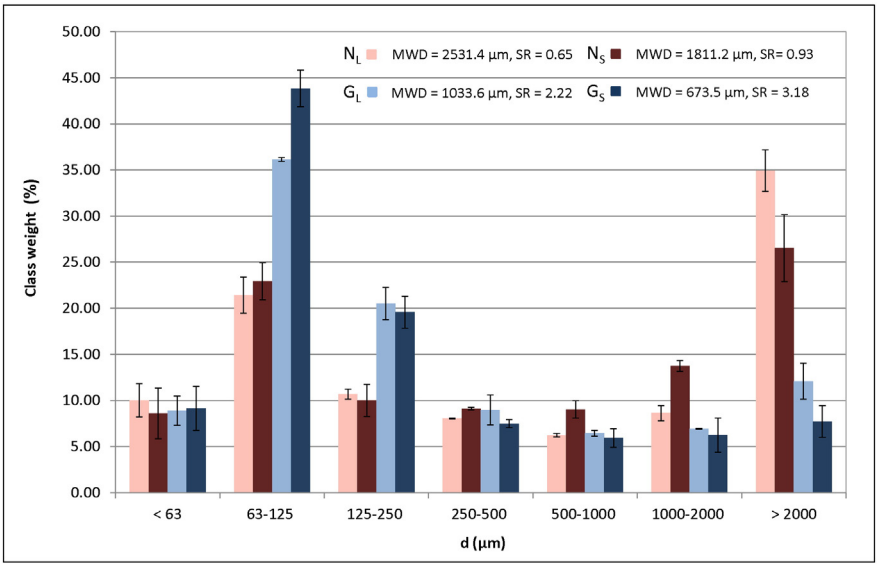

Fig. 2. Aggregate size distribution (ASD) of different initial soil aggregation states due to long-term (N_L, G_L) and short-term (N_S, G_S) impacts. Calculated MWD and SR values are presented at the top. S.D values are presented as bars (n = 18) on the columns.

in the amount of aggregates in the size range of 63–250 µm (saltators) following a decrease in the content of aggregates larger than 500 µm, depending on the initial soil aggregation state. The size fraction under 63 µm was not included in the calculation because this fraction is considered as dust which can be partly emitted by suspension and thus underestimation is expected. In the case of natural soils (N_L and N_S), there was a reduction only in the largest fraction (>2000 µm), especially in the short-term disturbed surfaces (N_S). In the grazing soils (G_L and G_S), the reduction in soil aggregation occurred also in the size fractions 1000–2000 µm (G_L and G_S) and 500–1000 µm (G_S). Thus soils with higher amounts of saltators in their initial ASD (Fig. 2), and respectively higher saltation impacts (Fig. 3), are associated with a higher rate of erosion of macro-aggregates (>500 µm) into saltators (Fig. 4). The erosion of larger aggregates can be related to the aggregation hierarchy concept (Tisdall and Oades, 1982; Six et al., 2004). It is suggested here that aggregates can breakdown due to the impact of other saltating grains and/or self-

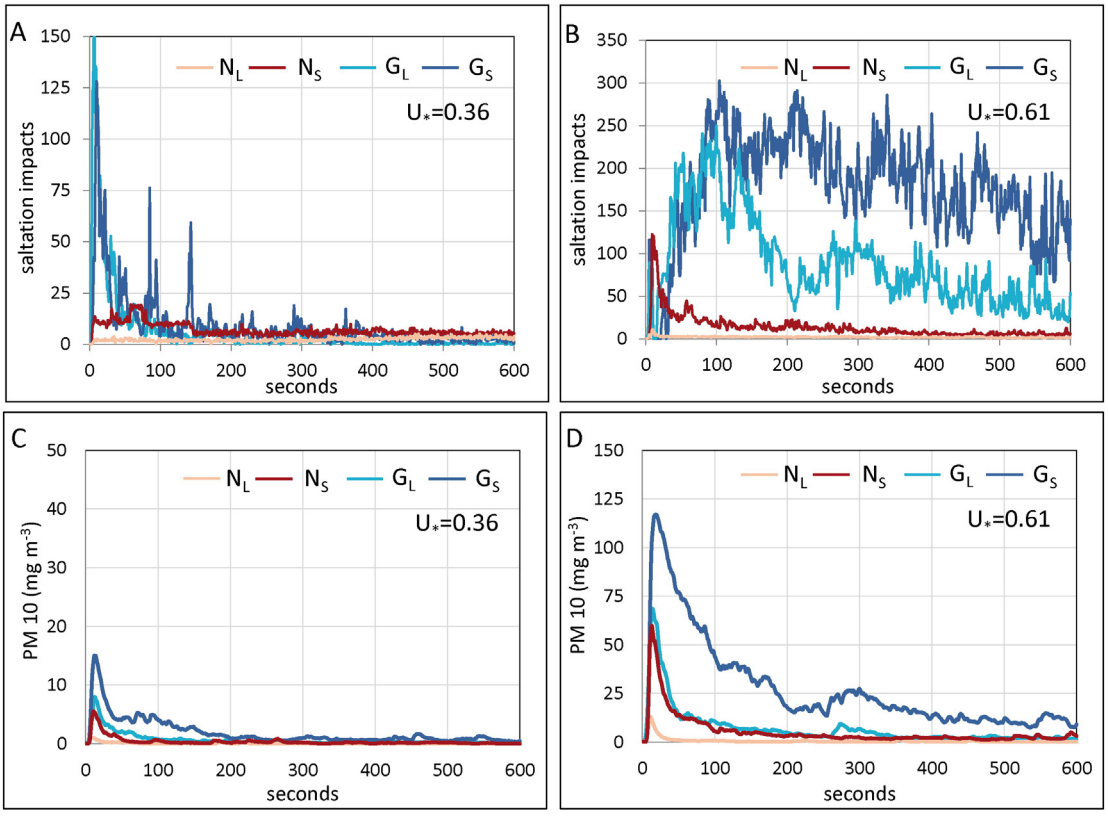

Fig. 3. Results of the aeolian experiments under shear velocities of 0.36 m s^{-1} and 0.61 m s^{-1}. The number of saltation impacts (A and B). PM_{10} concentrations over time (C and D). Note the differences in the scale of Y axes.

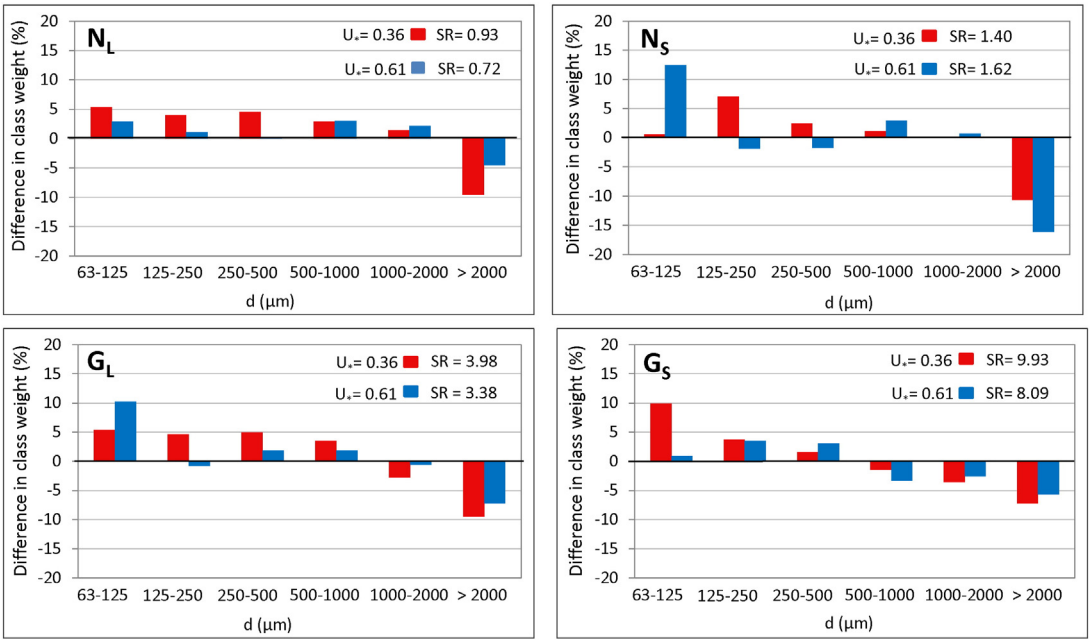

Fig. 4. Differences in the aggregate size distribution of topsoils following aeolian erosion. The values were calculated as the difference in the class weight of each size fraction before the experiment (Fig. 2) and after the experiment under two shear velocities (0.36 m s^{-1} and 0.61 m s^{-1}). The fraction <63 μm was not included due to the influence of dust suspension.

breakdown during saltation of the soil aggregates themselves (Kok et al., 2012).

The SR value following erosion under different shear velocities in the G_S soil (Fig. 4) was 2.5–3.1 fold higher compared with that of the initial ASD (Fig. 2), while in N_L the values were only 1.1–1.5 fold higher depending on the shear velocity. The higher shear velocity increased the amount of saltation and PM_{10} emission from all soils (Fig. 3). The results show no consistent trend in the production of saltators and/or breakdown of macro-aggregates (>500 μm) under the different shear velocities (Fig. 4). Under a low ASD, most of the aggregates can be transported already at the lower velocity of 0.36 m s^{-1} (~5 m s^{-1}) with limited amount of macro-aggregates that are available for erosion. Therefore,

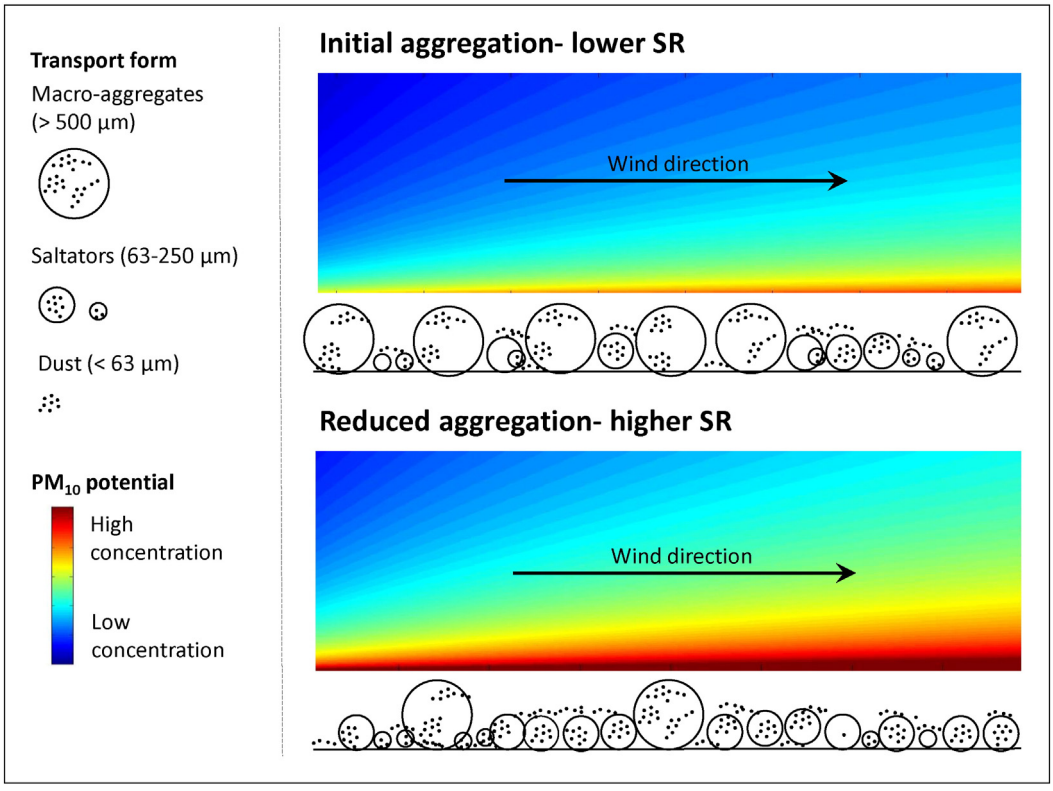

Fig. 5. Theoretical scheme of dust emission potential from the topsoil with relation to the aggregate size distribution. The soil aggregation is represented by SR values before and after aeolian erosion. The increase in SR value following erosion (lower plate) is associated with a higher rate of saltator production and dust emission.

maximum aeolian erosion of macro-aggregates, and thus saltator production, can be reached in such soils at low shear velocity.

3.3. Dust emission potential

The results of this study show that the dust concentrations and saltation rates are strongly influenced by the initial ASD of the topsoil (Fig. 3), where soils with lower initial ASD are associated with stronger aeolian transport. The aeolian erosion resulted in the breakdown of macro-aggregates into saltator-sized aggregates, leading to higher SR values (Fig. 4). Fig. 5 is a theoretical scheme illustrating the potential of dust emission from soils before and after erosion. The increase in SR values after erosion is assumed to influence the dust emission from the topsoil in the next wind event. We can expect that more saltators (higher SR) will result in higher dust emission rates.

Dust emission from the topsoil is considered as a complex process, which is controlled by numerous factors (Shao et al., 2011). Since in most dust sources the amount of loose particles on the surface is limited, dust emission of cohesive particles by direct lifting is enabled only under high wind velocities or under saltation flow (Bagnold, 1941; Kok et al., 2012). This is demonstrated in the positive relationships between the content of saltators (sand and/or aggregates), saltation rates, and dust emission (Houser and Nickling, 2001; Sweeney et al., 2011; Tanner et al., 2016). Thereby changes in the amount of saltators will have an influence on the dust production over time. This study suggests that the alteration in ASD during the aeolian erosion (Fig. 4) can increase the dust emission from the topsoil in the next wind event (Fig. 5). Considering that dust particles are an integral part of soil aggregates at all size levels, soil aggregation is a key factor in dust emission form source areas, and its dynamic property should be taken into consideration since the surface conditions at the start of a wind event will not persist for the duration of the event.

4. Conclusions

In this study we showed that soil aggregation changes due to aeolian erosion, with a perspective on the potential of dust emission from soils. PM emission and saltation rates depend on the initial aggregate size distribution as demonstrated in the aeolian experiments. The experiment results led to two major conclusions. First, the initial ASD of the soil changes due to aeolian processes – the content of saltators (63–250 μm) increases following breakdown of macro-aggregates (>500 μm). Second, the saltator production can change during the erosion process to increase the potential of dust emission from the soil in the next wind event. The findings provide an insight into soil aggregation as a key factor in determining soil erosion and dust emission potential. The soil dynamics should be implemented as soil parameterization in quantitative dust emission models from complex surfaces.

Acknowledgments

The study was supported by a grant from the Israel Science Foundation (1100/11) and Israel Binational Science Foundation (2014178). We thank Israel Chai Naveh for operating the aeolian experiments in the field, and two anonymous reviewers for their useful comments on the manuscript.

References

Abulaiti, A., Kimura, R., Shinoda, M., Kurosaki, Y., Mikami, M., Ishizuka, M., Yanada, Y., Nishihara, E., Gantsetseg, B., 2014. An observational study of saltation and dust emission in a hotspot of Mongolia. Aeolian Res. 15, 169–176.

Álvaro-Fuentes, J., Arrúe, J.L., Gracia, R., López, M.V., 2007. Soil management effects on aggregate dynamics in semiarid Aragon (NE Spain). Sci. Total Environ. 378 (1–2), 179–182.

Amézketa, E., 1999. Soil aggregate stability: a review. J. Sustain. Agric. 14 (2–3), 83–151.

Bacon, S.N., McDonald, E.V., Amit, R., Enzel, Y., Crouvi, O., 2011. Total suspended particulate matter emissions at high friction velocities from desert landforms. J. Geophys. Res. Earth Surf. (2003–2012) 116 (F3).

Bagnold, R.A., 1941. The Physics of Wind Blown Sand and Desert Dunes. Methuen, London (265,10).

Bissonnais, Y.L., 1996. Aggregate stability and assessment of soil crustability and erodibility: I. Theory and methodology. Eur. J. Soil Sci. 47 (4), 425–437.

Boix-Fayos, C., Calvo-Cases, A., Imeson, A.C., Soriano-Soto, M.D., 2001. Influence of soil properties on the aggregation of some Mediterranean soils and the use of aggregate size and stability as land degradation indicators. Catena 44 (1), 47–67.

Colazo, J.C., Buschiazzo, D.E., 2010. Soil dry aggregate stability and wind erodible fraction in a semiarid environment of Argentina. Geoderma 159 (1–2), 228–236.

Corp, I.B.M., 2011. IBM SPSS Statistics for Windows, Version 20.0. IBM Corp., Armonk, NY.

Hevia, G.G., Mendez, M., Buschiazzo, D.E., 2007. Tillage affects soil aggregation parameters linked with wind erosion. Geoderma 140 (1), 90–96.

Horn, R., Taubner, H., Wuttke, M., Baumgartl, T., 1994. Soil physical properties related to soil structure. Soil Tillage Res. 30 (2–4), 187–216.

Houser, C.A., Nickling, W.G., 2001. The emission and vertical flux of particulate matter <10 μm from a disturbed clay-crusted surface. Sedimentology 48 (2), 255–267.

Katra, I., Elperin, T., Fominykh, A., Krasovitov, B., Yizhaq, H., 2016. Modeling of particulate matter transport in atmospheric boundary layer following dust emission from source areas. Aeolian Res. 20, 147–156.

Klute, A., 1986. Methods of Soil Analysis. Part 1. Physical and Mineralogical Methods. American Society of Agronomy, Inc.

Kok, J.F., Parteli, E.J.R., Michaels, T.I., Karam, D.B., 2012. The physics of wind-blown sand and dust. Rep. Prog. Phys. 75 (10), 106901.

Krasnov, H., Katra, I., Novack, V., Vodonos, A., Friger, M.D., 2015. Increased indoor PM concentrations controlled by atmospheric dust events and urban factors. Build. Environ. 87, 169–176.

Lavee, H., Imeson, A.C., Sarah, P., 1998. The impact of climate change on geomorphology and desertification along a Mediterranean-arid transect. Land Degrad. Dev. 9 (5), 407–422.

Leys, J.F., Raupach, M.R., 1991. Soil flux measurements using a portable wind erosion tunnel. Aust. J. Soil Res. 29 (4), 533–552.

Masri, Z., Zobisch, M., Bruggeman, A., Hayek, P., Kardous, M., 2003. Wind erosion in a marginal Mediterranean dryland area: a case study from the Khanasser Valley, Syria. Earth Surf. Process. Landf. 28 (11), 1211–1222.

Pansu, M., Gautheyrou, J., 2006. Handbook of Soil Analysis: Mineralogical, Organic and Inorganic Methods. Springer.

Pinheiro, E.F.M., Pereira, M.G., Anjos, L.H.C., 2004. Aggregate distribution and soil organic matter under different tillage systems for vegetable crops in a red latosol from Brazil. Soil Tillage Res. 77 (1), 79–84.

Ravi, S., D'Odorico, P., Breshears, D.D., Field, J.P., Goudie, A.S., Huxman, T.E., Li, J., Okin, G.S., Swap, R.J., Thomas, A.D., Van Pelt, S., Whicker, J.J., Zobeck, T.M., 2011. Aeolian processes and the biosphere. Rev. Geophys. 49 (3).

Rice, M.A., Mullins, C.E., McEwan, I.K., 1997. An analysis of soil crust strength in relation to potential abrasion by saltating particles. Earth Surf. Process. Landf. 22 (9), 869–883.

Rowell, D.L., 1994. Soil Science: Methods and Applications. Longman Group Limited, Longman Scientific & Technical.

Shao, Y., 2008. Physics and Modelling of Wind Erosion vol. 37. Springer Science & Business Media, Berlin, Germany.

Shao, Y., Raupach, M.R., Findlater, P.A., 1993. Effect of saltation bombardment on the entrainment of dust by wind. J. Geophys. Res. Atmos. 98 (D7), 12719–12726.

Shao, Y., Wyrwoll, K.H., Chappell, A., Huang, J., Lin, Z., McTainsh, G.H., Mikami, M., Tanaka, T.Y., Wang, X., Yoon, S., 2011. Dust cycle: an emerging core theme in Earth system science. Aeolian Res. 2 (4), 181–204.

Sharratt, B., Wendling, L., Feng, G., 2010. Windblown dust affected by tillage intensity during summer fallow. Aeolian Res. 2 (2–3), 129–134.

Singh, P., Sharratt, B., Schillinger, W.F., 2012. Wind erosion and PM_{10} emission affected by tillage system in the world's driest rainfed wheat region. Soil Tillage Res. 124, 219–225.

Six, J., Bossuyt, H., Degryze, S., Denef, K., 2004. A history of research on the link between (micro) aggregates, soil biota, and soil organic matter dynamics. Soil Tillage Res. 79 (1), 7–31.

Spaccini, R., Piccolo, A., 2013. Effects of field managements for soil organic matter stabilization on water-stable aggregate distribution and aggregate stability in three agricultural soils. J. Geochem. Explor. 129, 45–51.

Sweeney, M., Etyemezian, V., Macpherson, T., Nickling, W., Gillies, J., Nikolich, G., McDonald, E., 2008. Comparison of PI-SWERL with dust emission measurements from a straight-line field wind tunnel. J. Geophys. Res. 113 (F1). http://dx.doi.org/10.1029/2007JF000830.

Sweeney, M.R., McDonald, E.V., Etyemezian, V., 2011. Quantifying dust emissions from desert landforms, eastern Mojave Desert, USA. Geomorphology 135 (1–2), 21–34.

Tanner, S., Katra, I., Haim, A., Zaady, E., 2016. Short-term soil loss by aeolian erosion in response to conventional and organic agricultural practices. Soil Tillage Res. 155, 146–156.

Tisdall, J.M., Oades, J.M., 1982. Organic matter and water-stable aggregates in soils. J. Soil Sci. 33 (2), 141–163.

Van Pelt, R.S., Baddock, M.C., Zobeck, T.M., Schlegel, A.J., Vigil, M.F., Acosta Martinez, V., 2013. Field wind tunnel testing of two silt loam soils on the North America Central high plains. Aeolian Res. 10, 53–59.

Vodonos, A., Friger, M., Katra, I., Krasnov, H., Zahger, D., Schwartz, J., Novack, V., 2015. Individual effect modifiers of dust exposure effect on cardiovascular morbidity. PLoS One 10 (9), e0137714.

Wang, X., Wang, J., Zhang, J., 2012. Comparisons of three methods for organic and inorganic carbon in calcareous soils of northwestern China. PLoS One 7 (8), e44334.

Wang, X., Cammeraat, E.L., Cerli, C., Kalbitz, K., 2014. Soil aggregation and the stabilization of organic carbon as affected by erosion and deposition. Soil Biol. Biochem. 72, 55–65.
Webb, N.P., Strong, C.L., 2011. Soil erodibility dynamics and its representation for wind erosion and dust emission models. Aeolian Res. 3 (2), 165–179.
Zaady, E., Yonatan, R., Shachak, M., Perevolotsky, A., 2001. The effects of grazing on abiotic and biotic parameters in semiarid ecosystem: a case study from the northern Negev desert, Israel. Arid Land Res. Manag. 15 (3), 245–261.
Zhang, S., Li, Q., Zhang, X., Wei, K., Chen, L., Liang, W., 2012. Effects of conservation tillage on soil aggregation and aggregate binding agents in black soil of Northeast China. Soil Tillage Res. 124, 196–202.
Zobeck, T.M., Popham, T.W., Skidmore, E.L., Lamb, J.A., Merrill, S.D., Lindstrom, M.J., Mokma, D.L., Yoder, R.E., 2013. Aggregate-mean diameter and wind-erodible soil predictions using dry aggregate-size distributions. Soil Sci. Soc. Am. J. 67 (2), 425–436.